RM H57E15a

NACA RM H57E15a

NACA

RESEARCH MEMORANDUM

EFFECT OF WING-MOUNTED EXTERNAL STORES ON THE LIFT AND DRAG OF THE DOUGLAS D-558-II RESEARCH AIRPLANE AT TRANSONIC SPEEDS

By Jack Nugent

High-Speed Flight Station
Edwards, Calif.

NATIONAL ADVISORY COMMITTEE
FOR AERONAUTICS

WASHINGTON

July 17, 1957

NATIONAL ADVISORY COMMITTEE FOR AERONAUTICS

RESEARCH MEMORANDUM

EFFECT OF WING-MOUNTED EXTERNAL STORES ON THE LIFT AND DRAG OF THE DOUGLAS D-558-II RESEARCH AIRPLANE AT TRANSONIC SPEEDS

By Jack Nugent

SUMMARY

A flight investigation was made of the Douglas D-558-II research airplane in both the basic and the 150-gallon DAC store configurations for a Mach number range from 0.48 to 1.03. Lift and drag values for both configurations are presented.

The addition of stores increased the drag at all Mach numbers tested. Below the drag rise the increase was of about the same magnitude as the increase in wetted area caused by the addition of the stores. Larger differences noted in the drag-rise region were probably due to a less favorable cross-sectional-area distribution. The addition of stores reduced the peak maximum lift-drag ratio by about 14 percent and reduced the drag-rise Mach number for lift coefficients of 0.2 and 0.4. For Mach numbers below about 0.93, the addition of stores increased the drag-due-to-lift factor. At a Mach number of 0.9 the basic configuration produced a drag-due-to-lift factor of 0.19, whereas the store configuration produced a value of about 0.24. There was little difference in the lift-curve slope C_{L_α} for the basic and store configurations for Mach numbers below about 0.8. Above 0.8, larger variations in C_{L_α} were noted for the store configuration. The basic configuration reached a peak C_{L_α} of about 0.09 at a Mach number of 0.8, whereas the store configuration reached a peak C_{L_α} of about 0.095 at a Mach number of 0.85.

INTRODUCTION

Since stores mounted externally at various airplane locations are being employed on present-day airplanes to increase fuel and armament capacity, determining the effects of these stores on the airplane's overall lift and drag characteristics has become of interest.

Wind-tunnel studies have been made comparing the lift and drag characteristics of basic and store-modified configurations for several airplanes, including a model of the Douglas D-558-II research airplane (refs. 1 to 3). However, little flight data exist on the effects of stores on the lift and drag coefficients of a full-scale airplane. Since the D-558-II airplanes were equipped to accommodate wing stores, a store-configuration flight program seemed advisable. However, only limited flight data were available for the lift and drag characteristics of the D-558-II (144) all-rocket airplane in the basic configuration (ref. 4). Therefore, at the request of the Bureau of Aeronautics, the NACA High-Speed Flight Station at Edwards, Calif., conducted flight tests of the Douglas D-558-II (145) turbojet- and rocket-powered research airplane both with and without external DAC fuel stores of 150 gallons capacity each mounted on pylons beneath the wings. This paper presents values of lift and drag coefficients for both configurations over a Mach number range from about 0.48 to about 1.03 within the usable lift range of the airplane. Data were obtained during push-down, pull-up maneuvers, accelerated turns, and speed runs covering an altitude range from about 20,000 feet to about 40,000 feet.

SYMBOLS

A	cross-sectional area, sq ft
A_e	exit area of rocket nozzle, sq in.
A_j	exit area of turbojet nozzle, sq in.
A_t	throat area of rocket nozzle, sq in.
a_n	measured normal acceleration, g units
a_x	measured longitudinal acceleration, g units
C_D	airplane drag coefficient
C_f	turbojet nozzle coefficient
C_L	airplane lift coefficient
C_{L_α}	slope of lift curve, deg^{-1}

C_r	rocket nozzle coefficient
dC_D/dC_L^2	drag-due-to-lift factor
F_i	inlet momentum of turbojet air, W_aV/g, lb
F_j	gross turbojet thrust, lb
F_r	rocket engine thrust, lb
g	acceleration due to gravity, ft/sec^2
h_p	pressure altitude, ft
$(L/D)_{max}$	maximum value of lift-drag ratio
l	length of airplane configuration, ft
M	free-stream Mach number
p_a	ambient static pressure, lb/sq ft abs
p_c	rocket chamber pressure, lb/sq in. abs
p_e	rocket nozzle exit pressure, lb/sq in. abs
p'_j	turbojet nozzle total pressure, lb/sq ft abs
q	free-stream dynamic pressure, lb/sq ft
S	wing area, sq ft
V	free-stream velocity, ft/sec
W	airplane weight, lb
W_a	engine air consumption, lb/sec
x	distance along fuselage from nose, ft
α	angle of attack of airplane center line, deg
θ	angle between turbojet thrust axis and airplane axis, deg

AIRPLANE AND STORES

The test airplane, one of the three Douglas D-558-II research airplanes, has the 30-percent chord of the unswept wing panel swept back 35°, sweptback tail surfaces, and an adjustable stabilizer for trim. The wing-leading edge slats were locked closed for the tests reported in this paper. The airplane is powered with a nonafterburning Westinghouse J34-WE-40 turbojet engine which exhausts out the bottom of the fuselage between the wing and the tail. Additional thrust is provided with a Reaction Motors LR8-RM-6 liquid rocket engine with a sea-level nominal thrust rating of 6,000 pounds available in four steps of 1,500 pounds each. Pertinent physical characteristics of the basic configuration are given in table I.

A three-view diagram of the D-558-II airplane showing the store configuration is given in figure 1 and a photograph of the airplane with stores is presented in figure 2. The stores tested were the Douglas DAC store shape of 150 gallons capacity and 180 inches in length. The stores were symmetrically mounted on pylons at about 61-percent wing semispan at predetermined wing-attach points. The thickness of the pylons was 7.6 percent. Four fins were originally mounted on each store in planes at 45° to the vertical. To insure adequate ground clearance during the flight tests, however, the fins were rotated to the vertical and horizontal planes and the bottom fin was removed. Details of the pylon and 150-gallon store are given in tables II and III, respectively, and mounting details are presented in figure 3.

INSTRUMENTATION

Standard NACA recording instruments were installed in the airplane to measure the following quantities pertinent to this investigation:

Airspeed
Altitude
Normal acceleration
Longitudinal acceleration
Angle of attack
Rocket cylinder combustion-chamber pressure
Turbojet engine speed
Turbojet nozzle total pressure
Compressor face total pressure
Elevator and stabilizer positions

All instruments were synchronized by a common timer.

An NACA high-speed pitot-static head with a type A-6 (ref. 5) total-pressure probe was mounted on a boom 57 inches forward of the nose of the airplane. The airspeed system was calibrated by the tower-pass method for Mach numbers below 0.8 and by the NACA radar-phototheodolite method for higher speeds (ref. 6). The angle of attack was measured from a vane mounted on the nose boom at a point 42 inches ahead of the nose of the airplane. Total pressures at the engine compressor face and jet nozzle were measured with cantilever-type probes inserted into the gas stream.

THRUST AND DRAG DETERMINATION

Thrust measurement was obtained both for the rocket engine and the turbojet engine to determine the lift and drag coefficients. For the rocket engine the following equation was used for each chamber of the engine firing:

$$F_r = p_c A_t C_r + A_e(p_e - p_a)$$

For the investigation, the values of C_r varied from 1.33 to 1.36 for individual cylinders as determined from ground runs at a thrust stand.

For the turbojet engine, sonic flow was established at the jet nozzle, permitting the use of the following equation for gross thrust:

$$F_j = C_f A_j(1.259p'_j - p_a)$$

The value of C_f was determined from ground runs at a thrust stand. A more detailed discussion of these equations is given in reference 7.

Ram drag was determined from the following equation:

$$F_i = \frac{W_a V}{g}$$

Engine air consumption was determined from pumping curves supplied by the engine manufacturer. Basic equations for the computation of the lift and drag coefficients are:

$$C_D = \frac{1}{qS}\left[W(a_n \sin\alpha - a_x \cos\alpha) + F_j \cos(\alpha + \theta) + F_r \cos\alpha - F_i\right]$$

$$C_L = \frac{1}{qS}\left[W(a_n \cos\alpha + a_x \sin\alpha) - F_j \sin(\alpha + \theta) - F_r \sin\alpha\right]$$

ACCURACY

The following accuracies of measurement are believed to be applicable for the results presented:

α, deg	±0.5
a_n, g	±0.025
a_x, g	±0.005
M	±0.01 subsonically ±0.02 transonically
q(M = 0.8, h_p = 37,500 ft), lb/sq ft	±3
W, lb	±100

All thrusts are accurate to ±150 lb.

A detailed discussion of the sources contributing to errors in measurement of these quantities is given in reference 7.

The error in lift coefficient is 5 percent or less throughout the lift range presented. The accuracy of the drag coefficient depends primarily on the accuracies of thrust, angle of attack, longitudinal acceleration, normal acceleration, weight, and Mach number. It is believed that the faired values of drag coefficient are accurate to within ±0.002 at low lift, since most of the aforementioned error sources are random.

TESTS, RESULTS, AND DISCUSSION

Lift and drag characteristics were determined for the Douglas D-558-II (145) research airplane in the clean condition for both the basic and the store configurations. The airplane was air-launched at about 30,000 feet from a Boeing B-29 mother airplane. Data were obtained over the altitude

range of about 20,000 feet to about 40,000 feet during climbing flight, speed runs, and turns. The higher speed data were obtained with both the rocket engine and the turbojet engine in operation. With the two engines operating, the ratio of rocket thrust to jet thrust was about 6 to 1 at the higher test altitudes. The Reynolds number of the tests varied from 12 to 20 million based on the wing mean aerodynamic chord. Use was made of the elevator or stabilizer, or both, during turns and for trim when the pilot found it necessary. Elevator position varied from 0° to 13.5°, trailing edge up; stabilizer position varied from 0.9° to 2.1°, trailing edge down for the test data used in this paper.

Figures 4 and 5 present the variation of lift coefficient with angle of attack and drag coefficient for several Mach numbers for both the basic and store configurations. Each curve presents data covering a narrow band of Mach number about the stated Mach number. Below the drag-rise Mach number the band was ±0.025; at higher Mach numbers it was reduced to ±0.01.

Figure 6 shows the data of figures 4 and 5 replotted for Mach numbers of about 0.50, 0.80, and 0.96. At a given lift coefficient for the test range, the addition of stores increased the angle of attack by about 1° for Mach numbers of 0.5 and 0.8; little effect was noted at a Mach number of about 0.95. The former result is probably associated with a reduction in local wing loading resulting from a decrease in positive pressure coefficients on the undersurface of the wing (ref. 8). The data also indicate the store configuration produced higher values of drag coefficient for all Mach numbers shown, with the largest difference indicated for a Mach number of 0.95.

The slopes of the lift curves of figures 4 and 5 are plotted against Mach number in figure 7 for lift coefficients below about 0.5 for the two configurations. There is little difference in C_{L_α} for Mach numbers below about 0.8 for the two configurations; above 0.8 larger variations in C_{L_α} were noted for the store configuration. The basic configuration reached a peak C_{L_α} of about 0.09 at $M = 0.8$, whereas the store configuration reached a peak C_{L_α} of about 0.095 at $M = 0.85$.

Figure 8 presents the variation of drag coefficient with Mach number for constant lift coefficients of 0.2, 0.4, and 0.6 obtained from the data of figures 4 and 5. In the subsonic region the curves show a relatively constant level of drag coefficient before drag rise. For all lift coefficients in this region the drag for the store configuration exceeded that for the basic configuration with an increase of about 20 percent in C_D at $M = 0.8$ and $C_L = 0.2$. The addition of the stores and pylons added about 18 percent to the wetted area of the basic configuration. This result suggests the increased drag is due to skin-friction effects. In the drag-rise region the difference in drag coefficient between the two configurations increases. This latter condition may be

the result, in part, of the less favorable cross-sectional-area distribution effected by the addition of the stores. As shown in figure 9, the addition of the store and pylon results in a more abrupt change in cross-sectional area in the region of the wing, tending to increase the drag according to the area rule (ref. 9).

Returning to figure 8, the curves indicate a reduction in drag-rise Mach number $\left(\frac{dC_D}{dM} = 0.1\right)$ with the addition of stores for lift coefficients of 0.2 and 0.4. Data from reference 2 are shown in figure 8 for comparison purposes at $M = 0.85$ and $C_L = 0.2$ for the basic and store configurations. The wind-tunnel data indicate essentially the same drag penalty due to store addition as measured in flight.

Figure 10 presents the variation with Mach number of $(L/D)_{max}$ and of C_L for $(L/D)_{max}$ for the data of figures 4 and 5. The basic configuration produced a higher value of $(L/D)_{max}$ for all Mach numbers where direct comparison can be made. The basic configuration produced a peak $(L/D)_{max}$ of about 11.4, whereas the store configuration produced a peak value of about 9.8, both peaks occurring at a Mach number of about 0.75. This represents a reduction of approximately 14 percent in peak $(L/D)_{max}$. Correspondingly, the basic configuration produced a lower value of C_L for $(L/D)_{max}$ for Mach numbers below about 0.98.

Figure 11 presents C_L^2 plotted against C_D using data from figures 4 and 5. Straight lines were faired through the data for lift coefficients less than 0.55. The slope of a straight line so obtained is a measure of the drag due to lift for the lift-coefficient range from 0 to 0.55 and is referred to as the drag-due-to-lift factor dC_D/dC_L^2. Figure 12 shows the variation of drag-due-to-lift factor for both the basic configuration and the store configuration for the test Mach number range. For the basic configuration there is a steady increase in dC_D/dC_L^2 as Mach number increases from about 0.5 to 0.96, suggesting a large decrease in wing leading-edge suction as transonic speeds are approached. The store configuration shows a higher value of dC_D/dC_L^2 for all Mach numbers tested below 0.93. Above this value the reverse is true. At a Mach number of 0.9 the basic configuration produced a value of dC_D/dC_L^2 of 0.19, whereas the store configuration produced a value of about 0.24.

CONCLUSIONS

Flight tests of the lift and drag of the Douglas D-558-II (145) research airplane in the basic and 150-gallon DAC store configurations

for a Mach number range of 0.48 to 1.03 led to the following conclusions:

1. The addition of stores increased the drag at all Mach numbers tested. Below the drag rise the increase was of about the same magnitude as the increase in wetted area caused by the addition of the stores. Larger differences noted in the drag-rise region were probably due to a less favorable cross-sectional-area distribution.

2. The addition of stores reduced the peak lift-drag ratio $(L/D)_{max}$ by about 14 percent and reduced the drag-rise Mach number for lift coefficients of 0.2 and 0.4.

3. For Mach numbers below about 0.93 the addition of stores increased the drag-due-to-lift factor dC_D/dC_L^2. At a Mach number of 0.9 the basic configuration produced a value of dC_D/dC_L^2 of 0.19, whereas the store configuration produced a value of about 0.24.

4. There was little difference in lift-curve slope C_{L_α} for the basic and store configurations for Mach numbers below about 0.8. Above 0.8, larger variations in C_{L_α} were noted for the store configuration. The basic configuration reached a peak lift-curve slope of about 0.09 at a Mach number of 0.8, whereas the store configuration reached a peak lift-curve slope of about 0.095 at a Mach number of 0.85.

High-Speed Flight Station,
National Advisory Committee for Aeronautics,
Edwards, Calif., April 23, 1957.

REFERENCES

1. Smith, Norman F.: Exploratory Investigation of External Stores on the Aerodynamic Characteristics of a 1/16-Scale Model of the Douglas D-558-II Research Airplane at a Mach Number of 2.01. NACA RM L54F02, 1954.

2. Silvers, H. Norman, and King, Thomas J., Jr.: Investigation at High Subsonic Speeds of the Effects of Various Underwing External-Store Arrangements on the Aerodynamic Characteristics of a 1/16-Scale Model of the Douglas D-558-II Research Airplane. NACA RM L55D11, 1955.

3. Kelly, Thomas C.: Transonic Wind-Tunnel Investigation of the Effects of External Stores and Store Position on the Aerodynamic Characteristics of a 1/16-Scale Model of the Douglas D-558-II Research Airplane. NACA RM L55I07, 1955.

4. Nugent, Jack: Lift and Drag Characteristics of the Douglas D-558-II Research Airplane Obtained in Exploratory Flights to a Mach Number of 2.0. NACA RM L54F03, 1954.

5. Gracey, William, Letko, William, and Russell, Walter R.: Wind-Tunnel Investigation of a Number of Total-Pressure Tubes at High Angles of Attack. Subsonic Speeds. NACA TN 2331, 1951. (Supersedes NACA RM L50G19.)

6. Zalovcik, John A.: A Radar Method of Calibrating Airspeed Installations on Airplanes in Maneuvers at High Altitudes and at Transonic and Supersonic Speeds. NACA Rep. 985, 1950. (Supersedes NACA TN 1979.)

7. Beeler, De E., Bellman, Donald R., and Saltzman, Edwin J.: Flight Techniques for Determining Airplane Drag at High Mach Numbers. NACA TN 3821, 1956.

8. Hallissy, Joseph M., Jr., and Kudlacik, Louis: A Transonic Wind-Tunnel Investigation of Store and Horizontal-Tail Loads and Some Effects of Fuselage-Afterbody Modifications on a Swept-Wing Fighter Airplane. NACA RM L56A26, 1956.

9. Smith, Norman F., Bielat, Ralph P., and Guy, Lawrence D.: Drag of External Stores and Nacelles at Transonic and Supersonic Speeds. NACA RM L53I23b, 1953.

TABLE I

PHYSICAL CHARACTERISTICS OF THE BASIC

DOUGLAS D-558-II AIRPLANE

Wing:	
Root airfoil section (normal to 30-percent chord of unswept panel)	NACA 63-010
Tip airfoil section (normal to 30-percent chord of unswept panel)	NACA 63_1-012
Total area, sq ft	175.0
Span, ft	25.0
Mean aerodynamic chord, in.	87.301
Root chord (parallel to plane of symmetry), in.	108.51
Tip chord (parallel to plane of symmetry), in.	61.18
Taper ratio	0.565
Aspect ratio	3.570
Sweep at 30-percent chord of unswept panel, deg	35.0
Sweep of leading edge, deg	38.8
Incidence at fuselage center line, deg	3.0
Dihedral, deg	-3.0
Geometric twist, deg	0
Total aileron area (rearward of hinge line), sq ft	9.8
Aileron travel (each), deg	±15
Total flap area, sq ft	12.58
Flap travel, deg	50
Horizontal tail:	
Root airfoil section (normal to 30-percent chord of unswept panel)	NACA 63-010
Tip airfoil section (normal to 30-percent chord of unswept panel)	NACA 63-010
Area (including fuselage), sq ft	39.9
Span, in.	143.6
Mean aerodynamic chord, in.	41.75
Root chord (parallel to plane of symmetry), in.	53.6
Tip chord (parallel to plane of symmetry), in.	26.8
Taper ratio	0.50
Aspect ratio	3.59
Sweep at 30-percent chord line of unswept panel, deg	40.0
Dihedral, deg	0
Elevator area, sq ft	9.4
Elevator travel, deg	
Up	25
Down	15
Stabilizer travel, deg	
Leading edge up	4
Leading edge down	5
Vertical tail:	
Airfoil section (normal to 30-percent chord of unswept panel)	NACA 63-010
Area, sq ft	36.6
Height from fuselage center line, in.	98.0
Root chord (parallel to fuselage center line), in.	146.0
Tip chord (parallel to fuselage center line), in.	44.0
Sweep angle at 30-percent chord of unswept panel, deg	49.0
Rudder area (rearward of hinge line), sq ft	6.15
Rudder travel, deg	±25
Fuselage:	
Length, ft	42.0
Maximum diameter, in.	60.0
Fineness ratio	8.40
Speed-retarder area, sq ft	5.25
Engines:	
Turbojet	J34-WE-40
Rocket	LR8-RM-6
Airplane weight, lb:	
Full jet and rocket fuel	15,570
Full jet fuel	12,382
No fuel	10,822

TABLE II

DIMENSIONS OF PYLON USED WITH DOUGLAS EXTERNAL STORES (150 GAL. TANK)

[Stations and ordinates given in inches]

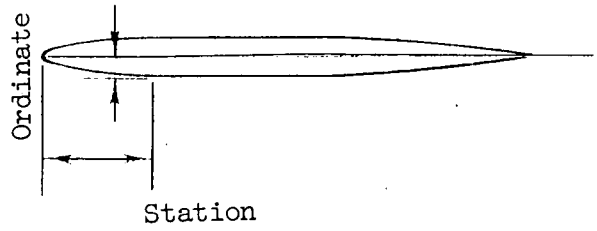

Station	Ordinate	Station	Ordinate
0	0	30.00	2.500
.5	.513	32.5	2.500
1.0	.718	35.0	2.500
2.5	1.111	37.5	2.500
5.0	1.528	38.5	2.500
7.5	1.821	41.0	2.481
10.0	2.043	43.5	2.419
12.5	2.213	46.0	2.308
15.0	2.341	48.5	2.147
17.5	2.430	51.0	1.936
20.0	2.482	53.5	1.677
22.5	2.500	58.5	1.048
25.0	2.500	63.5	.342
27.5	2.500	66.0	0

L.E. radius: 0.275
T.E. radius: 0.045

TABLE III

DIMENSIONS OF 150-GALLON DOUGLAS FUEL TANK

[Stations and radii given in inches]

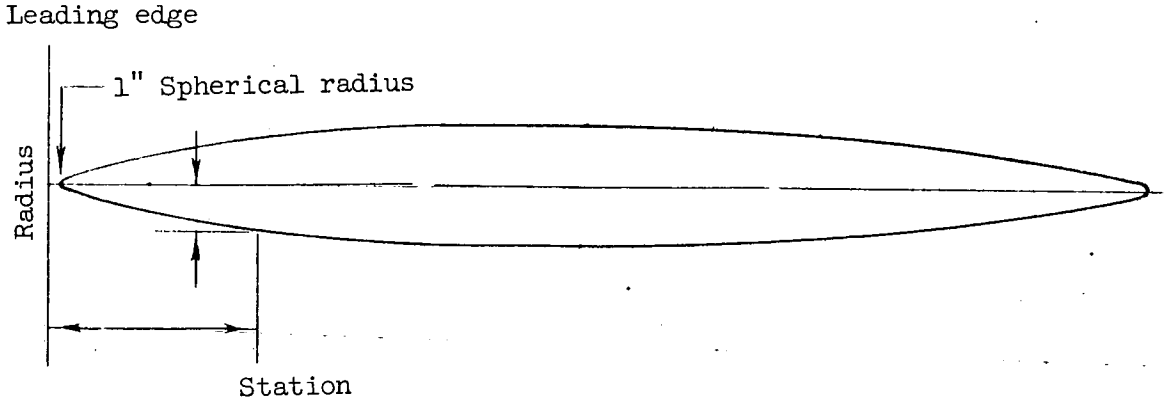

Station	Radius	Station	Radius
0	0	109.5	9.912
6	2.745	119.5	9.225
13.5	5.165	129.5	8.322
23.5	7.228	139.5	7.242
33.5	8.541	148.0	6.215
43.5	9.489	153.0	5.575
53.5	10.190	158.0	4.917
63.5	10.500	163.0	4.246
73.5	10.500	168.5	3.500
83.5	10.500	172.5	2.934
89.5	10.500	176.5	2.174
99.5	10.348	180.0	0
L.E. slope: Tan = 0.531 T.E. radius: 1.000			

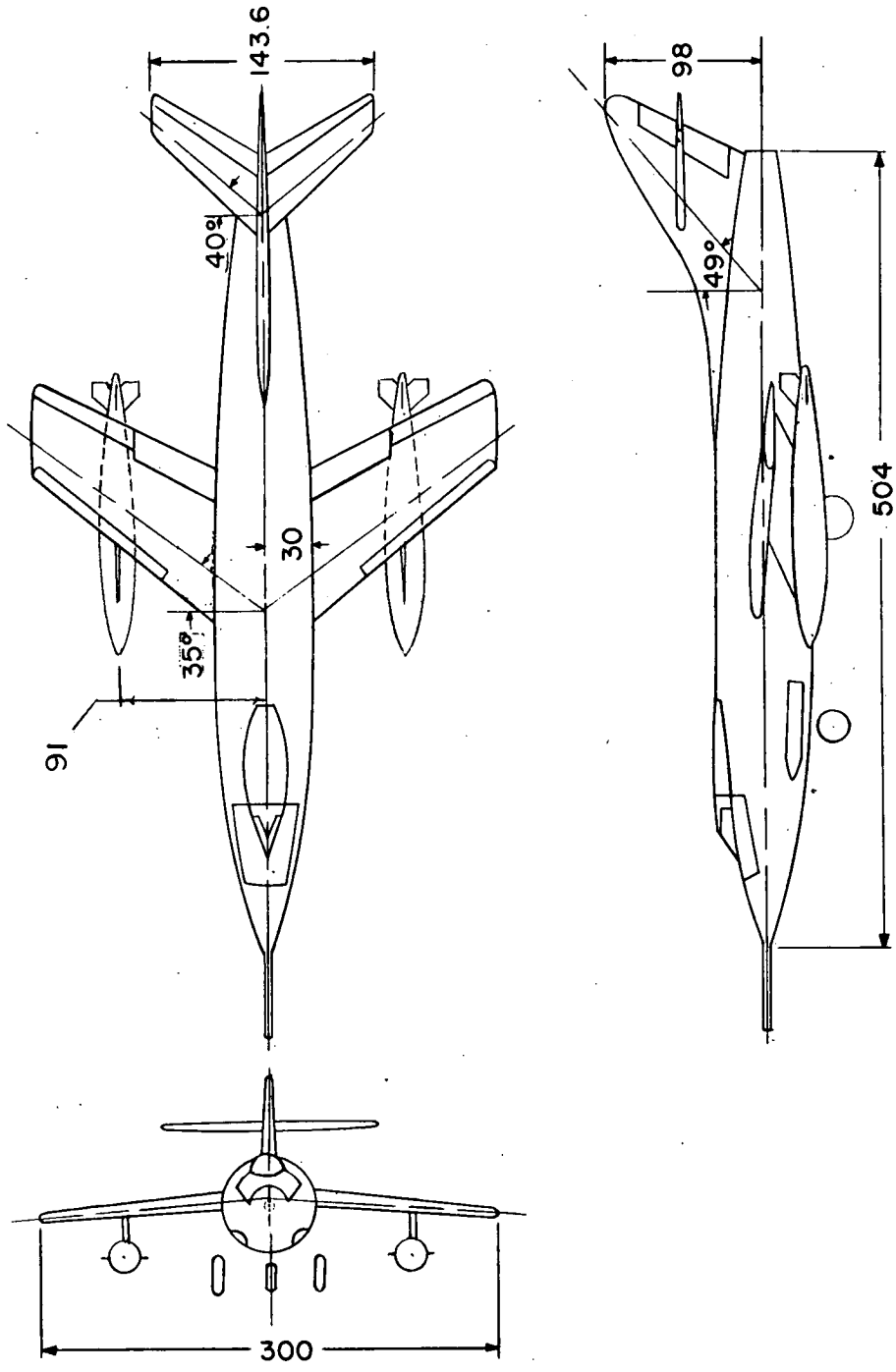

Figure 1.- Three-view drawing of the Douglas D-558-II research airplane showing installation of the DAC 150-gallon external stores. All dimensions in inches.

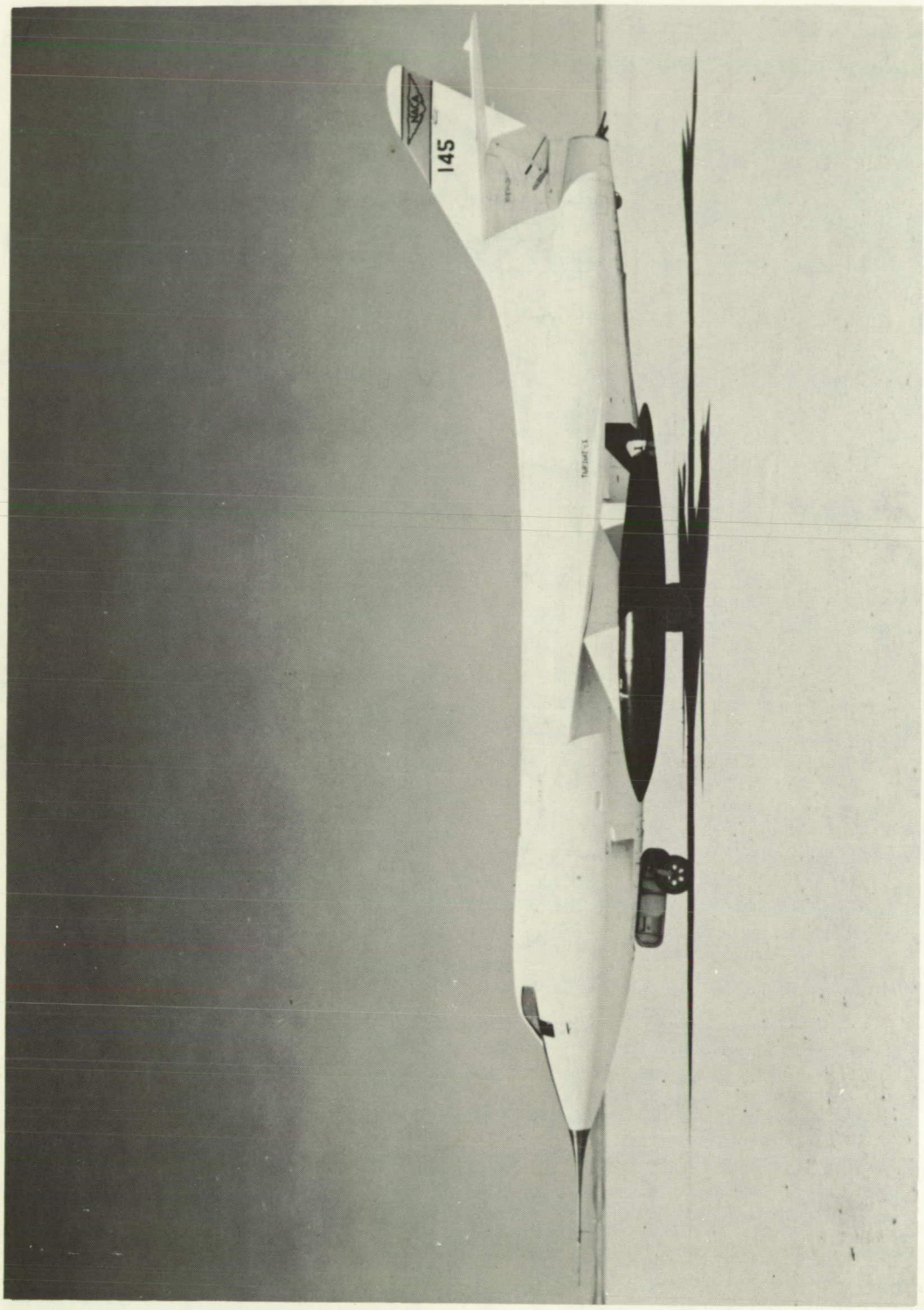

Figure 2.- Photograph of the external-store configuration. E 1861

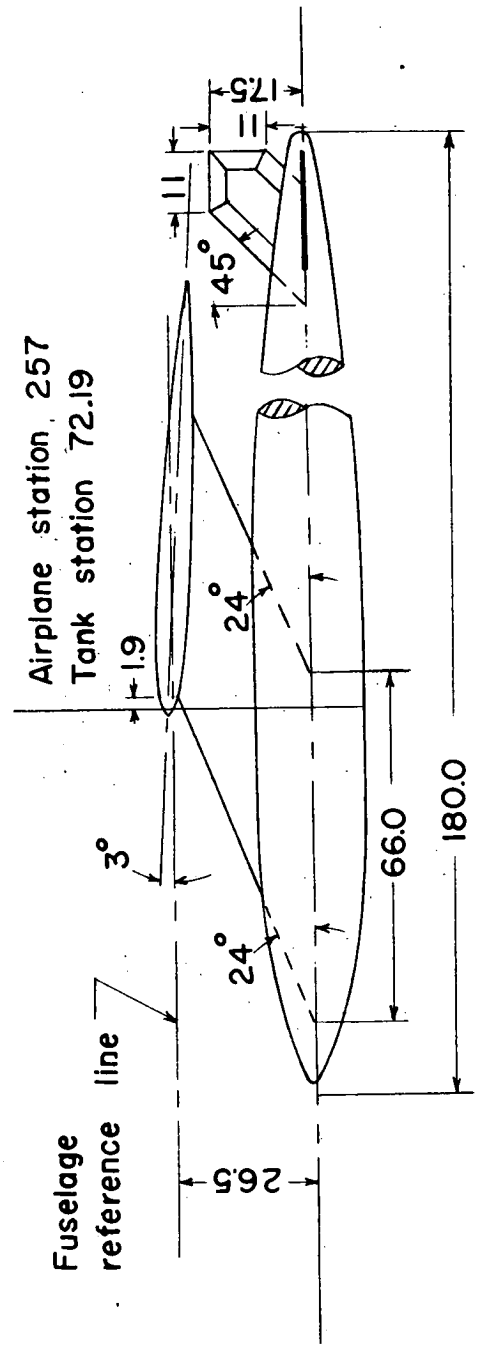

Figure 3.- External store configuration for D-558-II airplane using 150-gallon DAC stores. All dimensions in inches.

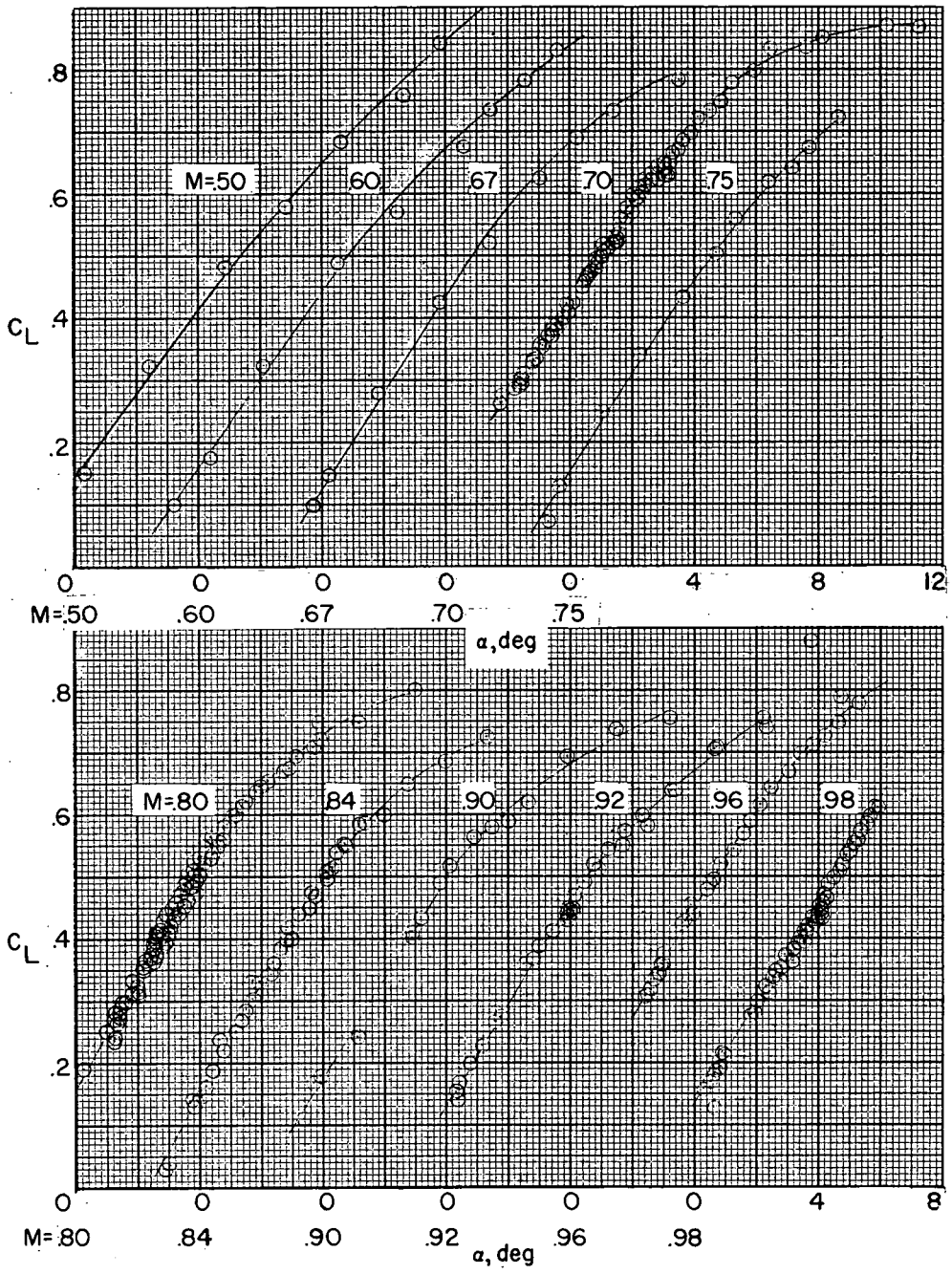

(a) C_L plotted against α.

Figure 4.- Variation of lift coefficient with angle of attack and with drag coefficient for basic configuration for several Mach numbers.

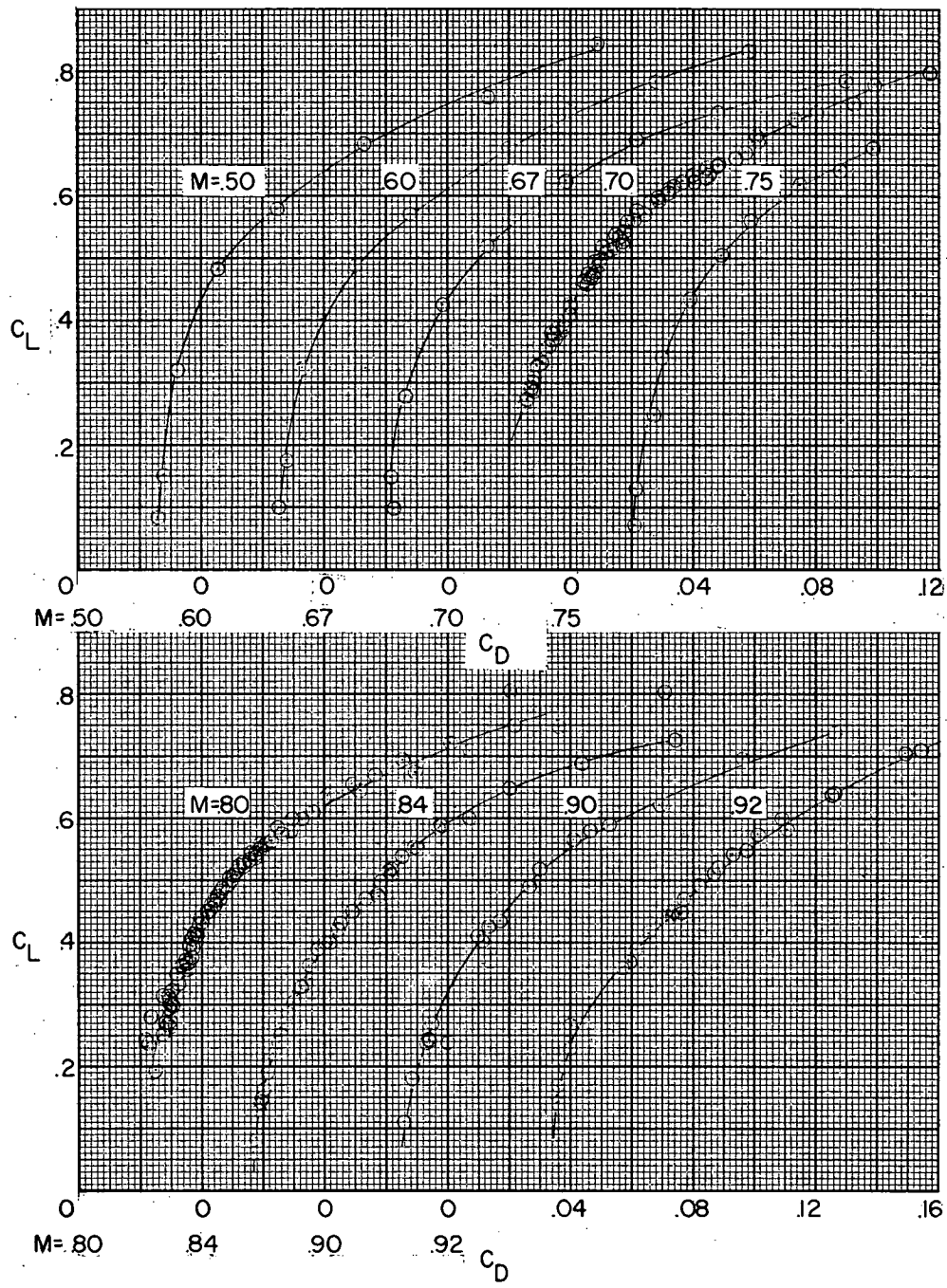

(b) C_L plotted against C_D.

Figure 4.- Continued.

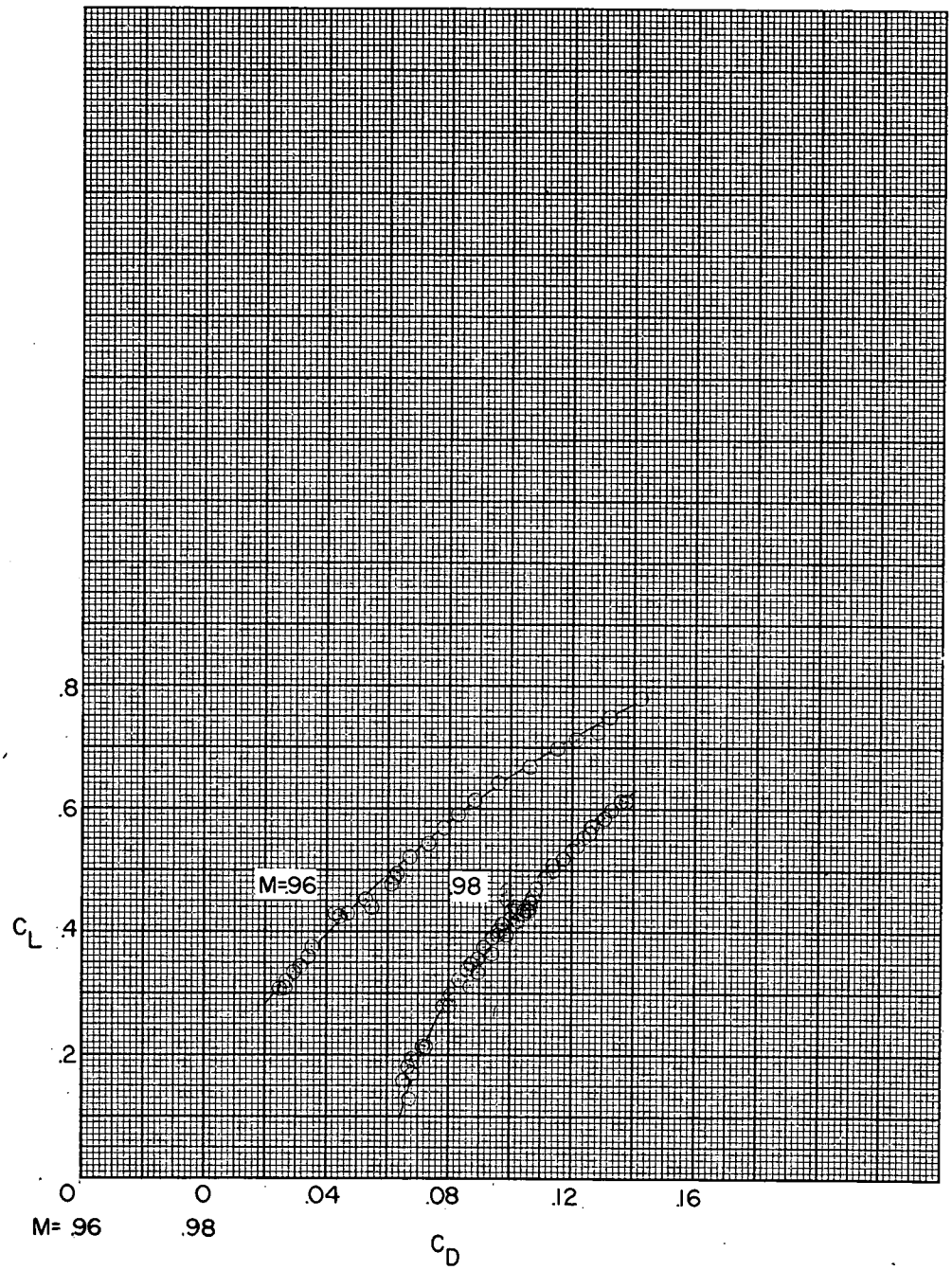

(b) Concluded.

Figure 4.- Concluded.

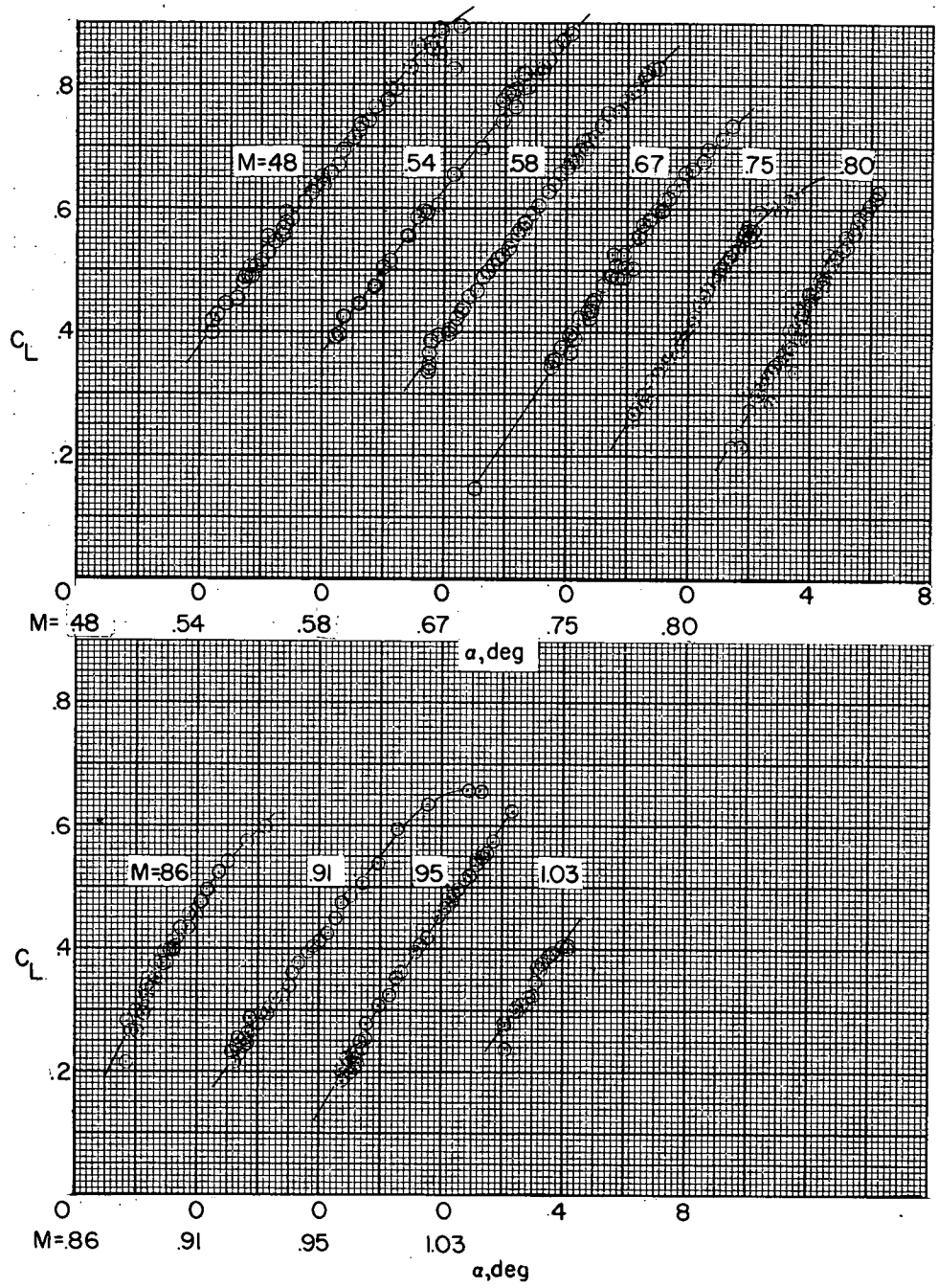

(a) C_L plotted against α.

Figure 5.- Variation of lift coefficient with angle of attack and with drag coefficient for store configuration for several Mach numbers.

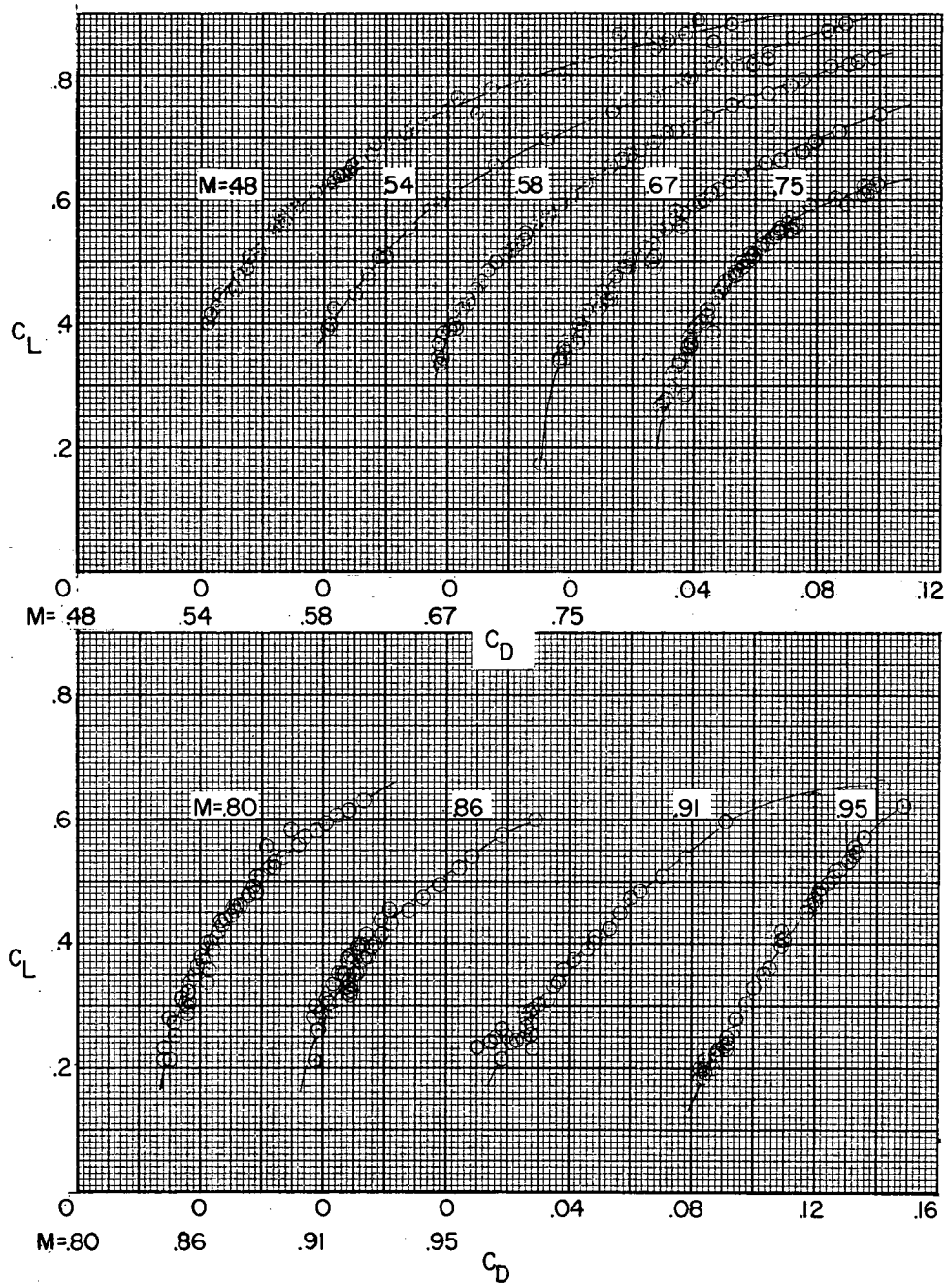

(b) C_L plotted against C_D.

Figure 5.- Continued.

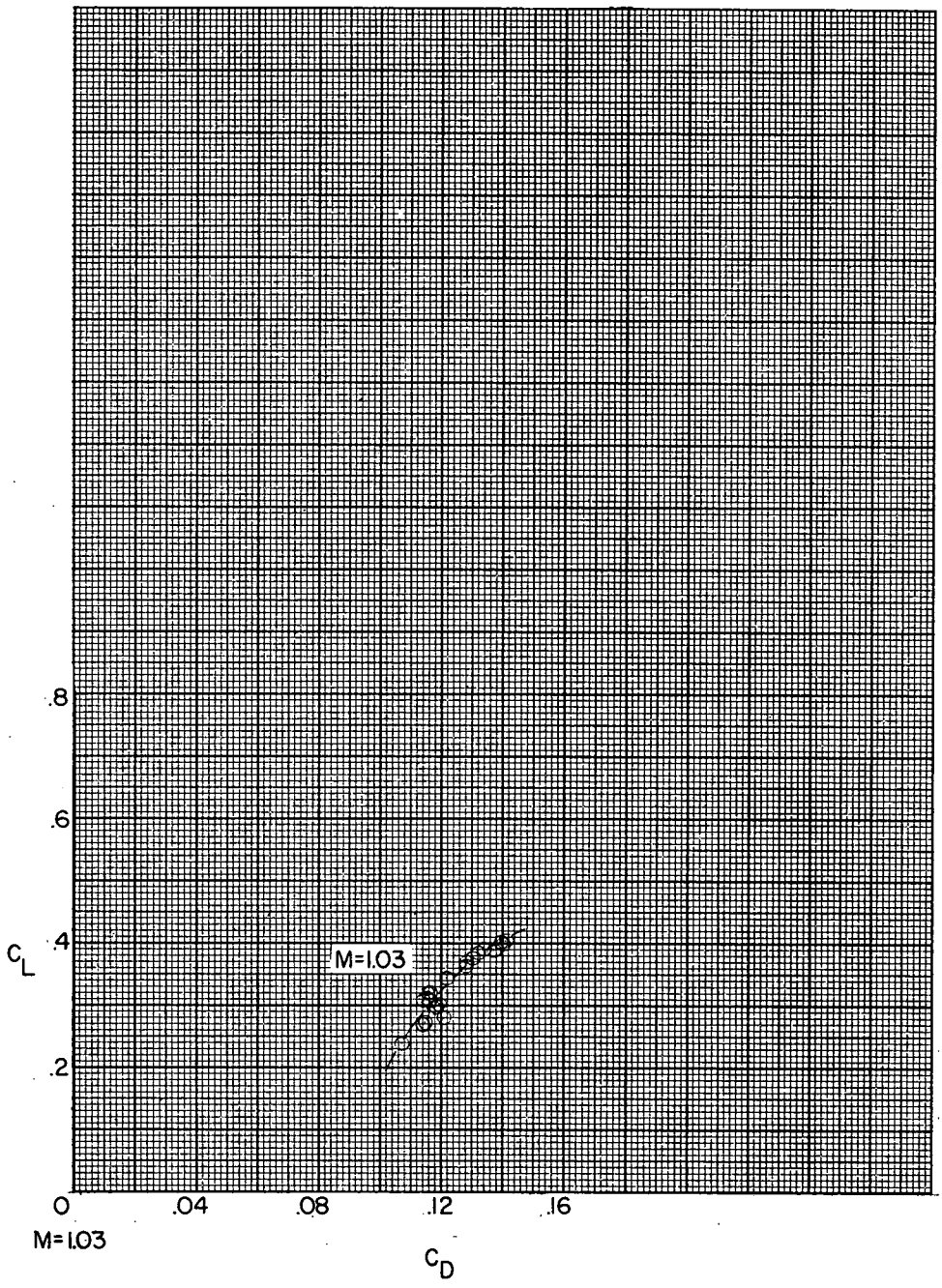

(b) Concluded.

Figure 5.- Concluded.

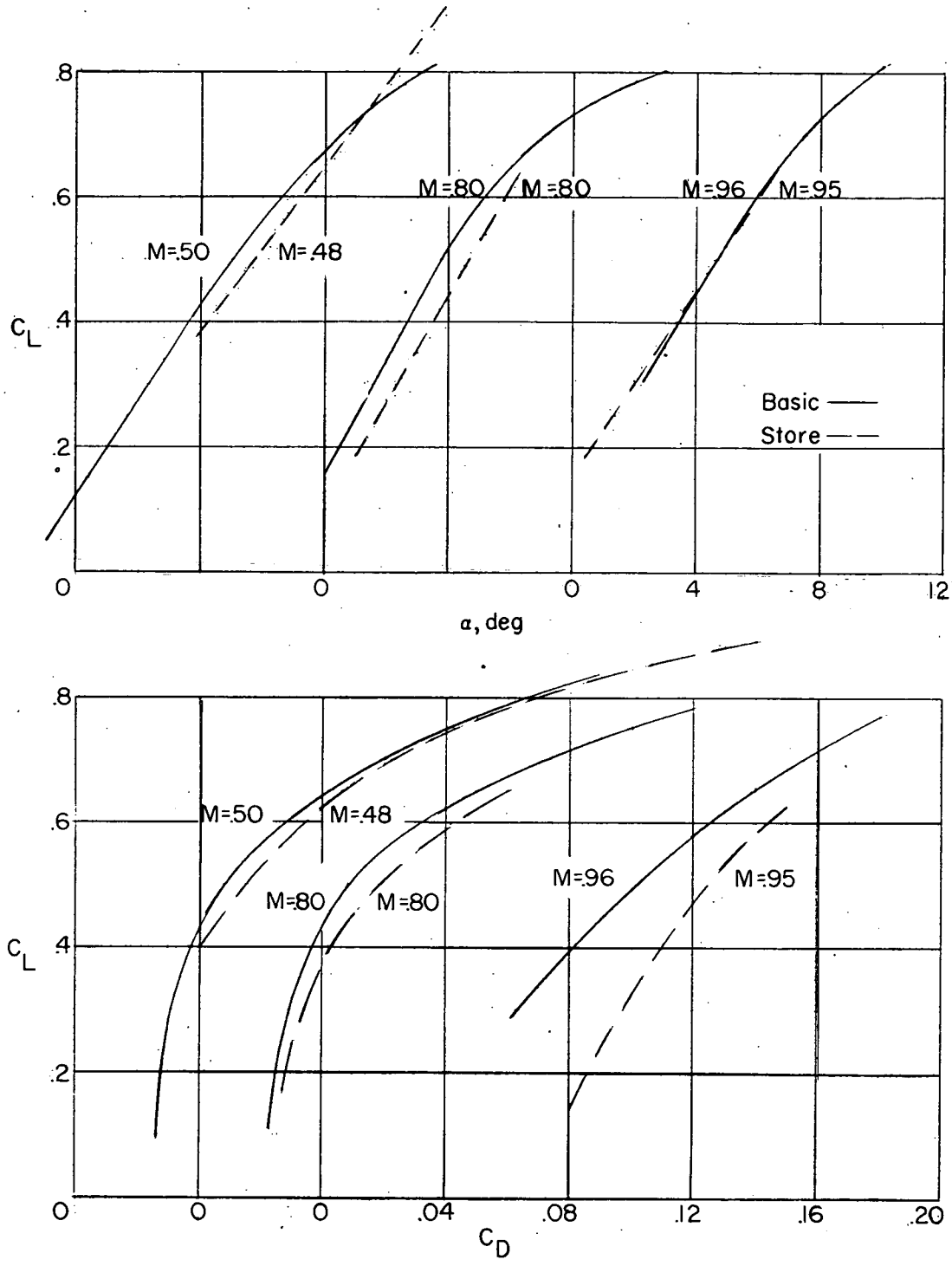

Figure 6.- Comparison of lift curves and polar curves for several Mach numbers.

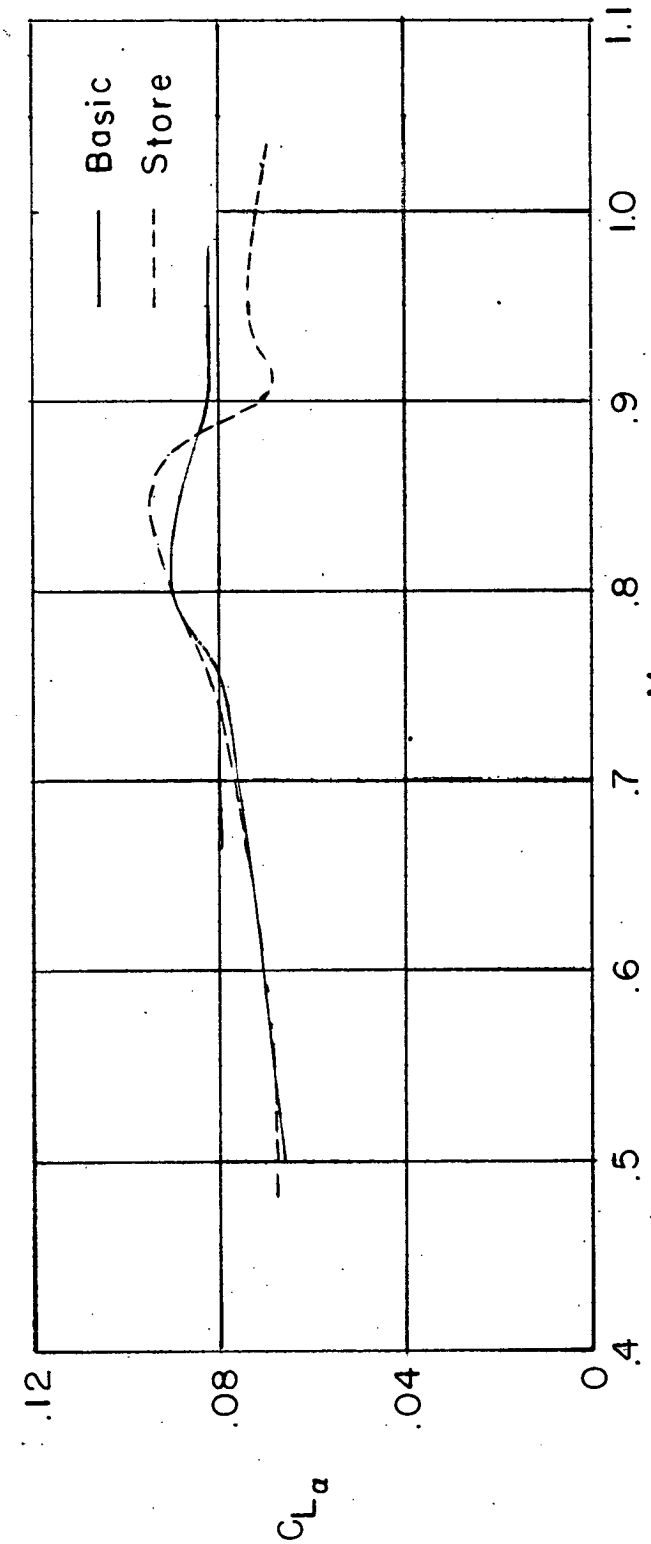

Figure 7.- Variation of lift-curve slope with Mach number; $C_L < 0.5$.

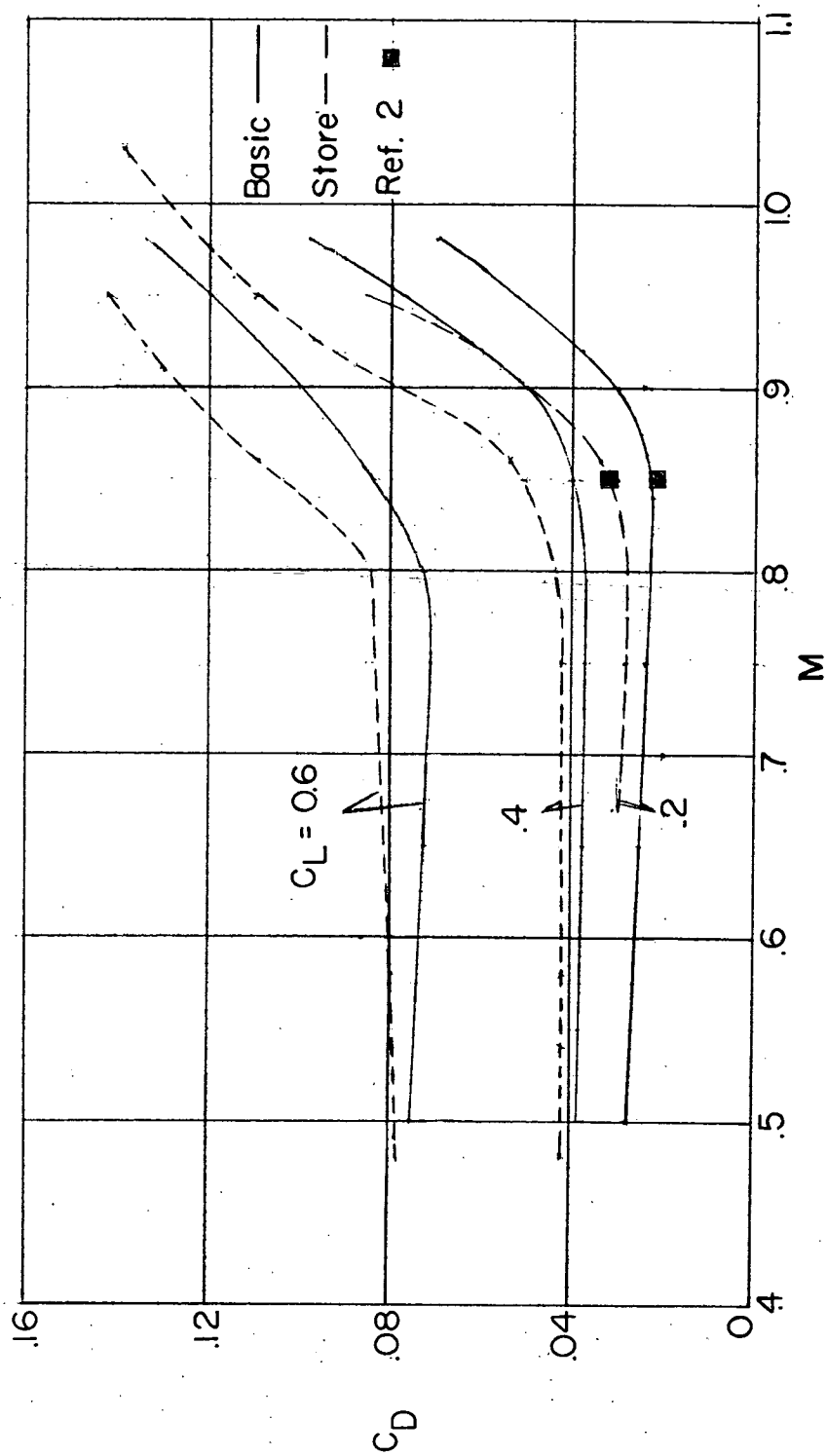

Figure 8.- Variation of C_D with M for several lift coefficients.

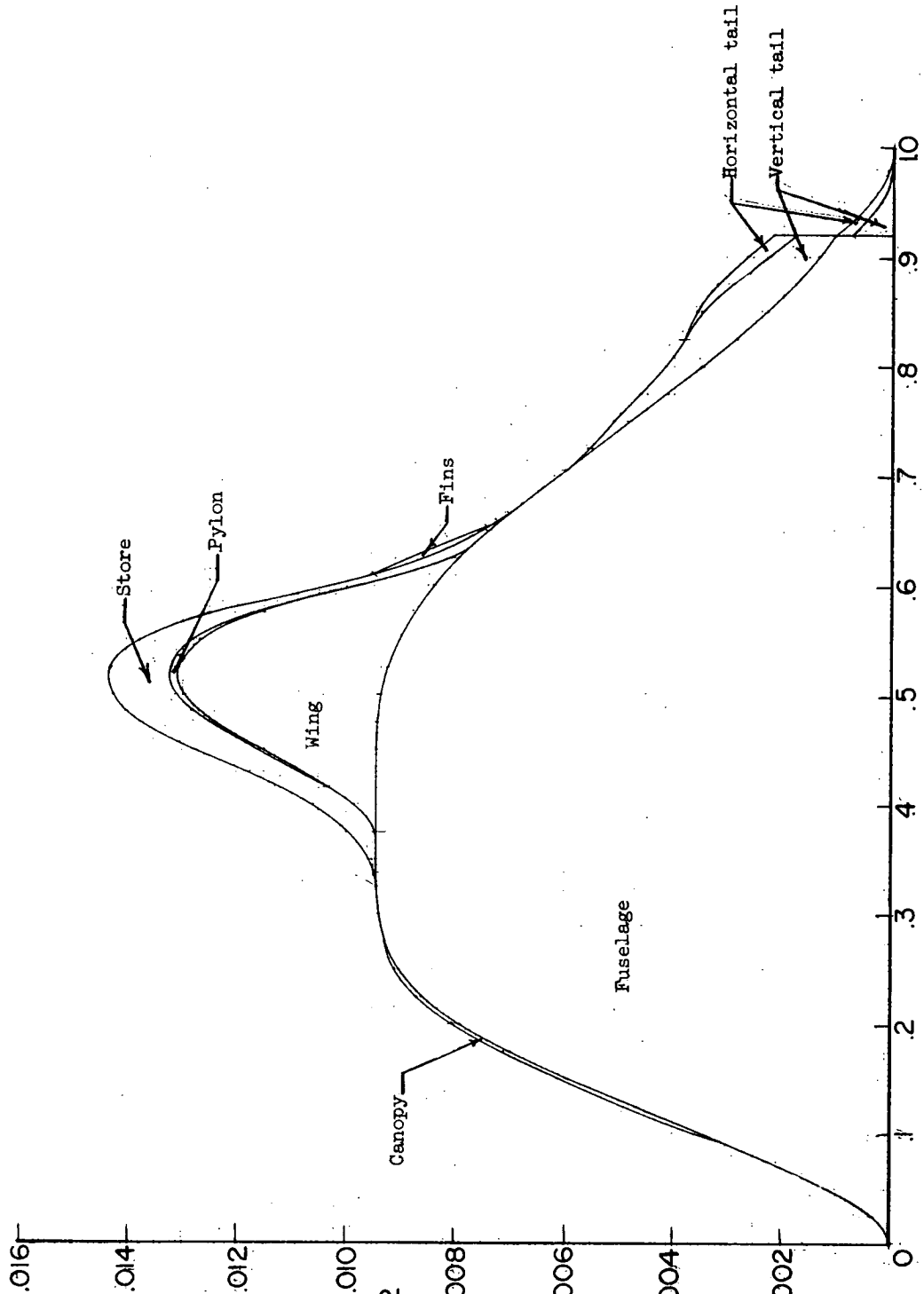

Figure 9.- Cross-sectional area distribution for basic and store configurations.

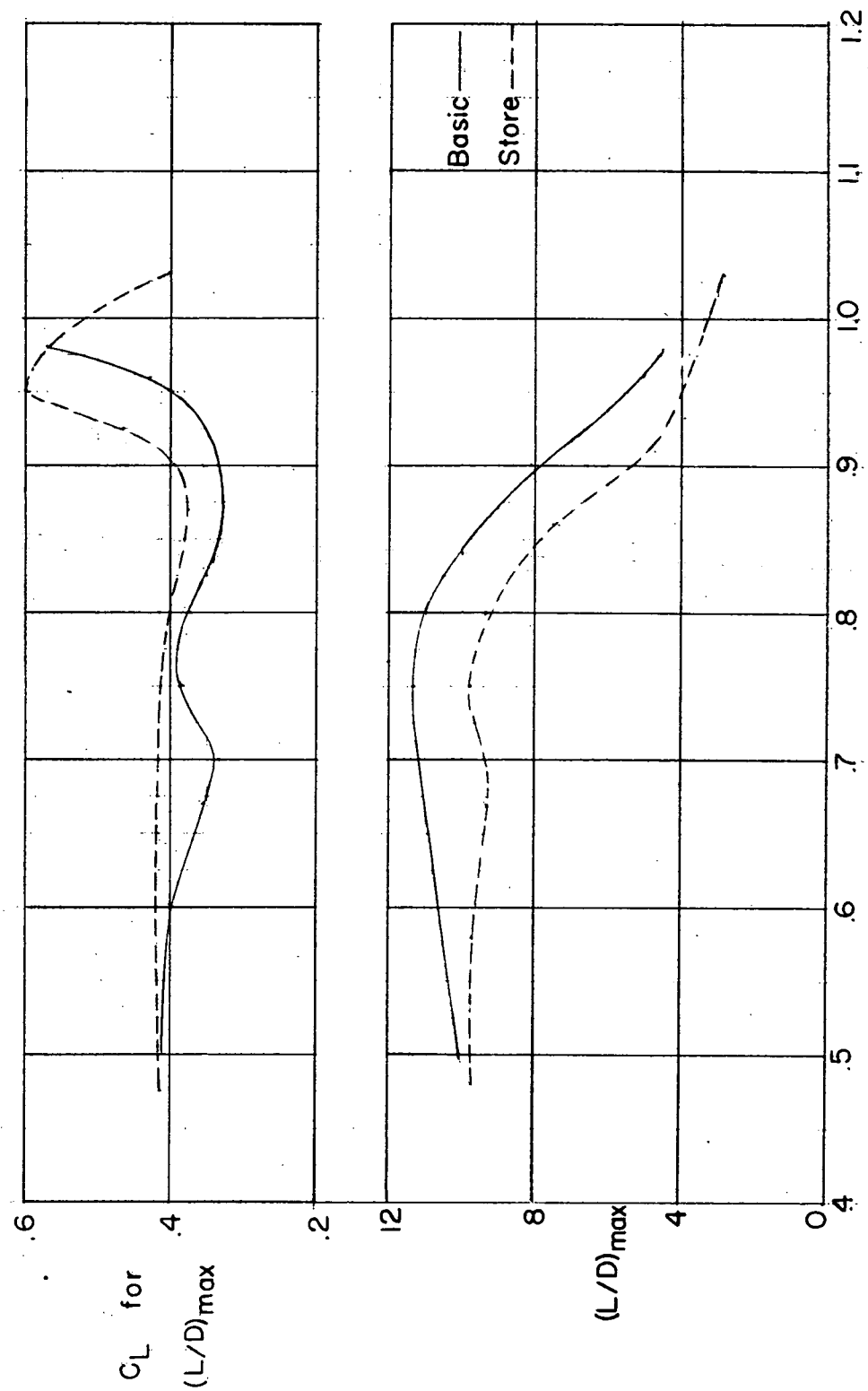

Figure 10.- Variation of $(L/D)_{max}$ and C_L for $(L/D)_{max}$ with Mach number.

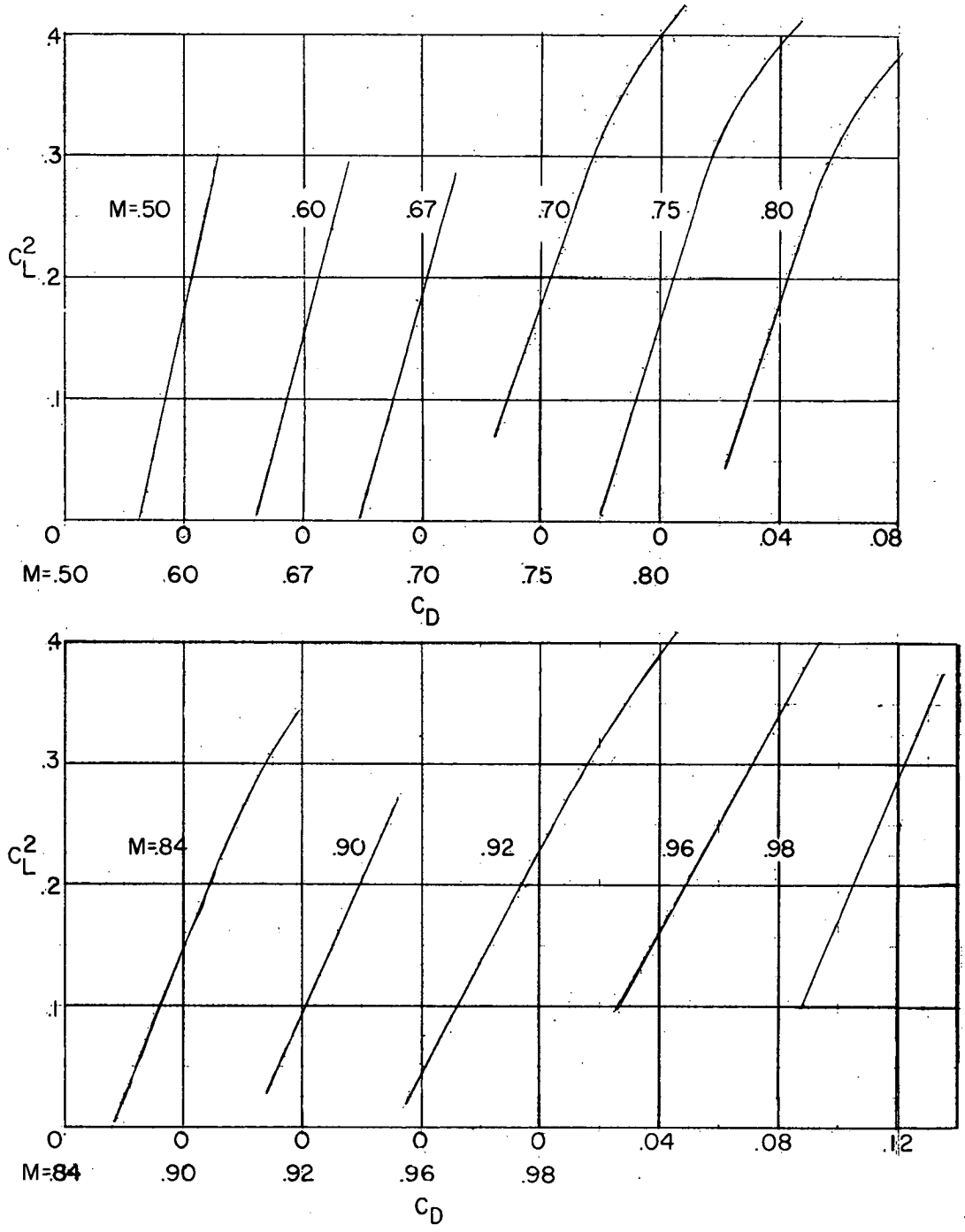

(a) Basic configuration.

Figure 11.- C_L^2 plotted against C_D for several Mach numbers.

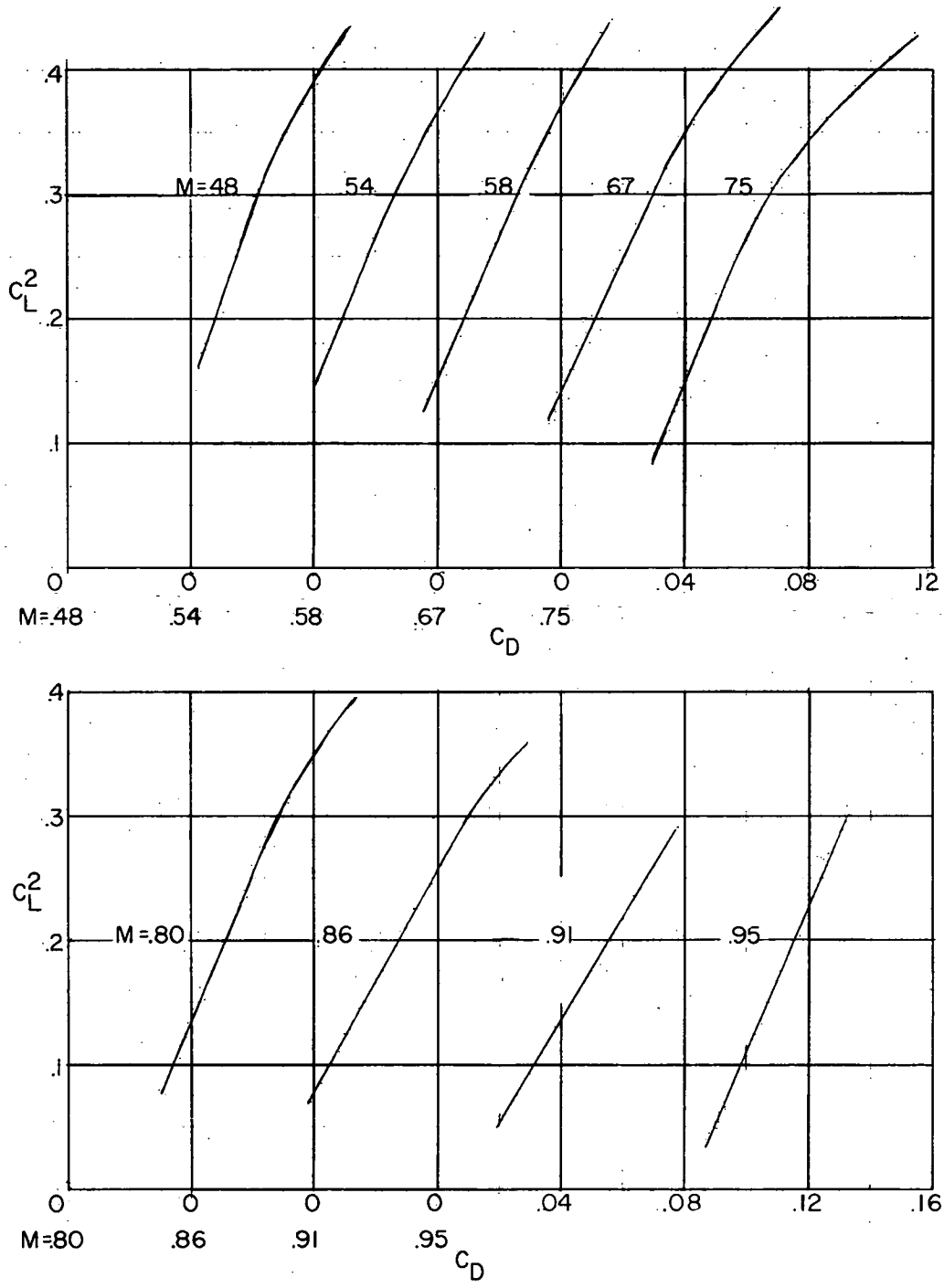

(b) Store configuration.

Figure 11.- Concluded.

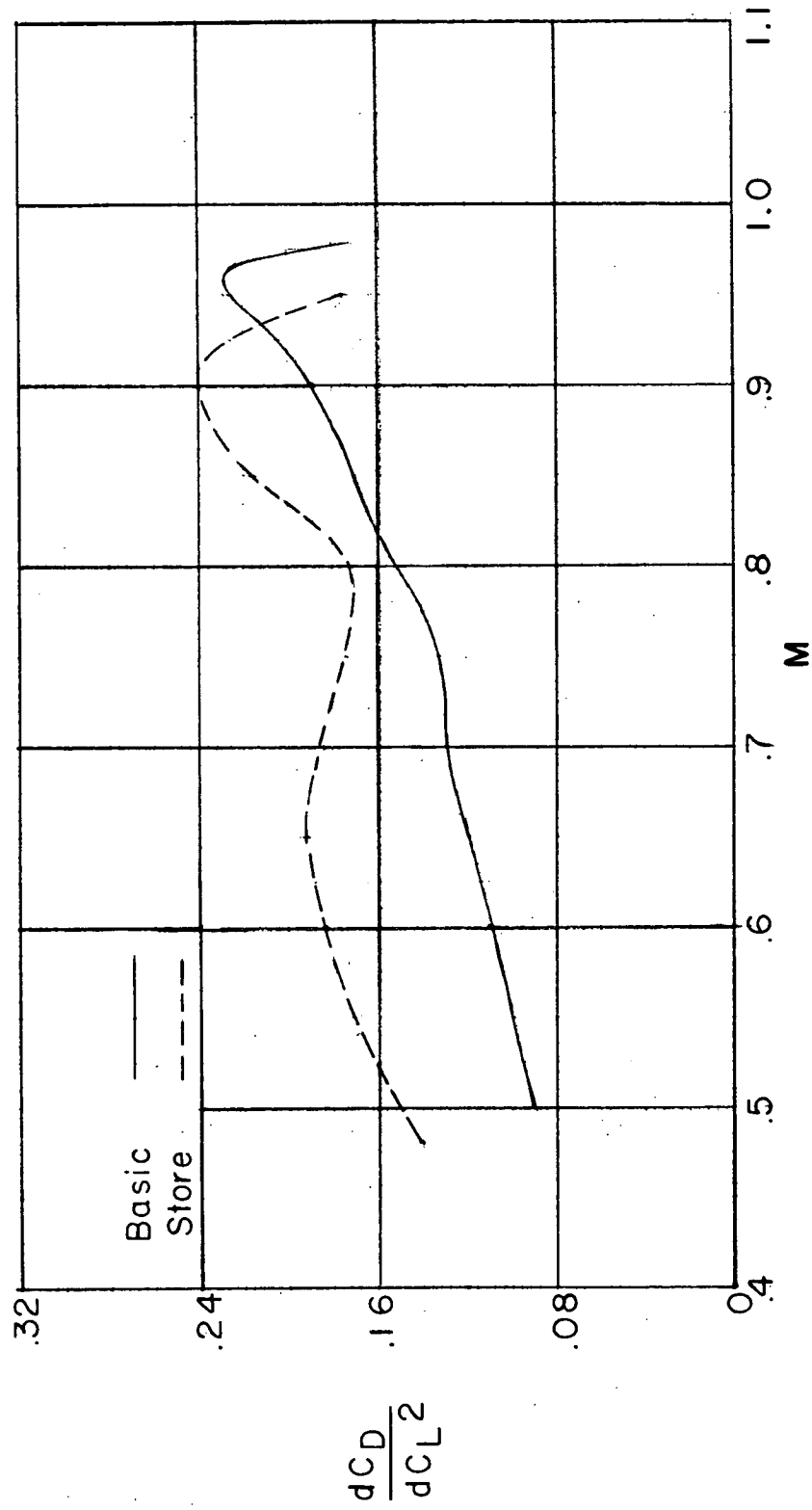

Figure 12.- Variation of drag-due-to-lift factor with Mach number.

NACA - Langley Field, Va.